

Production of charmonium states in heavy ion collisions

Heavy Ion Meeting
2015-05

May 16th 2015

Pusan National University



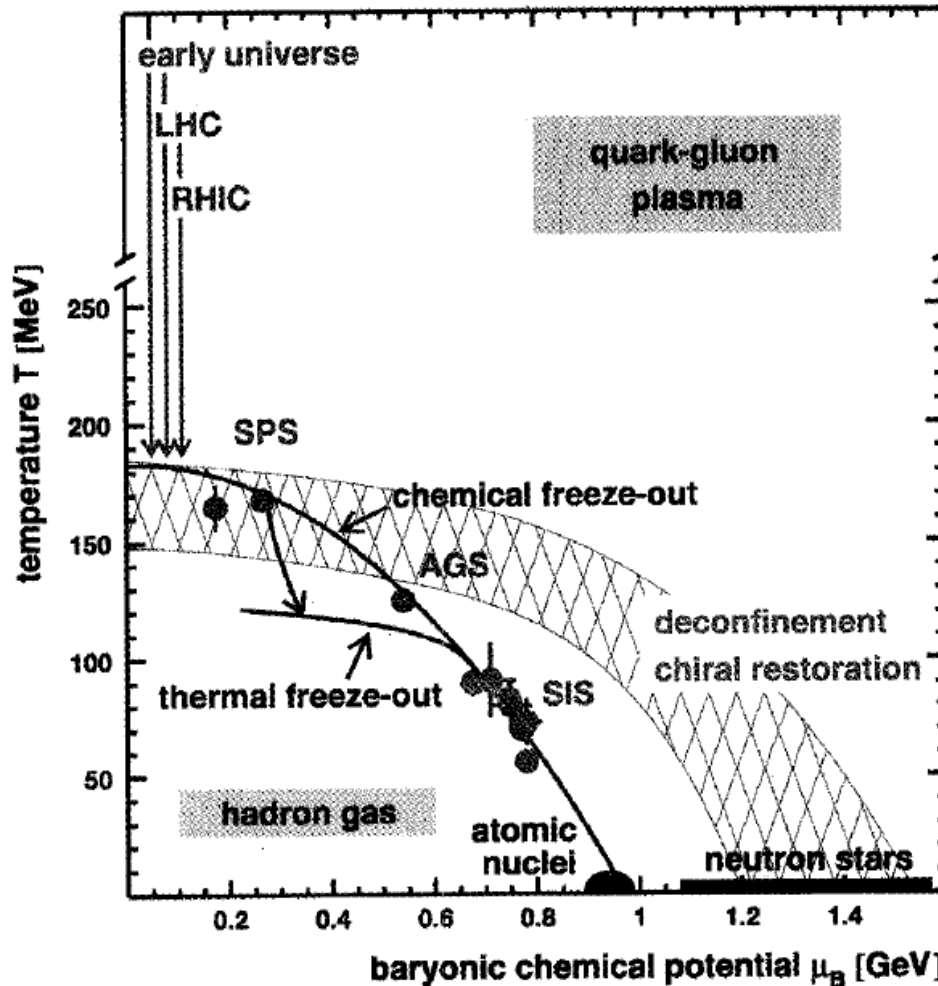
Sungtae Cho
Kangwon National University

Outline

- Introduction
- Charmonium states
- Hadron production
- Charmonium states in heavy ion collisions
- Conclusion

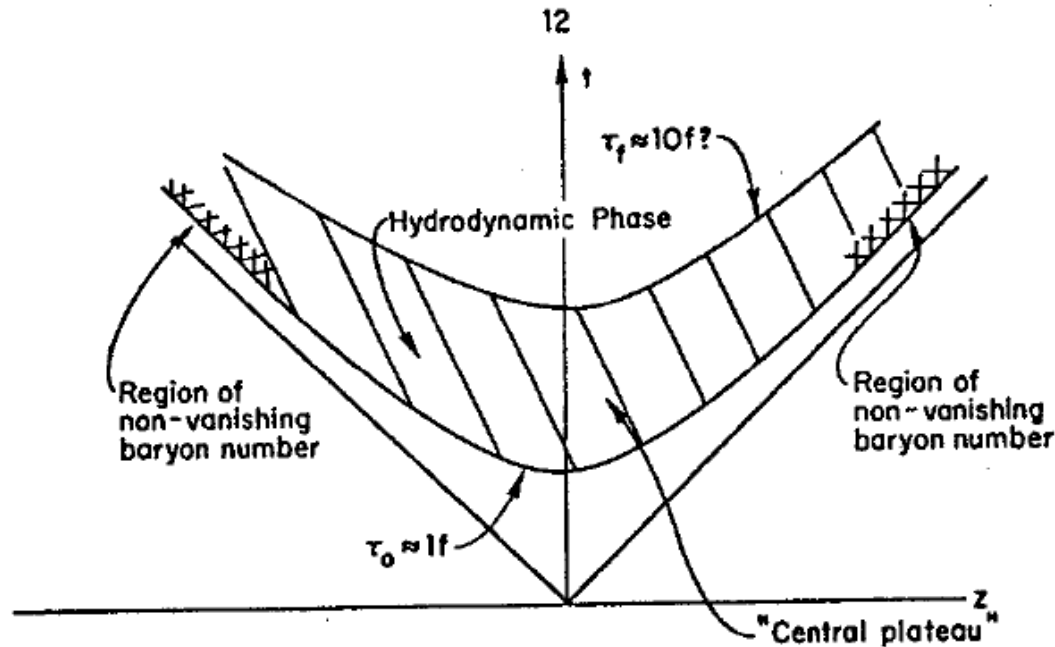
Introduction

– QCD phase diagram



P. Braun-Munzinger
and J. Stachel, Nucl. Phys.
A **690**, 119c (2001)

– Time evolution of quark-gluon plasma



$$\tau = \sqrt{t^2 - z^2}$$

J. D. Bjorken, Phys. Rev. D **27**, 140 (1983)

- i. Collision
- ii. Pre-equilibrium state and Quark-gluon plasma
- iii. Hydrodynamic expansion
- iv. Chemical freeze-out
- v. Kinetic freeze-out

Charmonium states

– Quarkonia

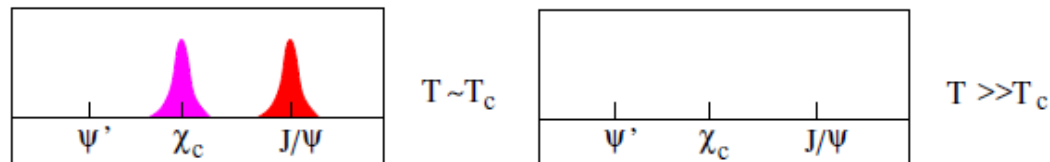
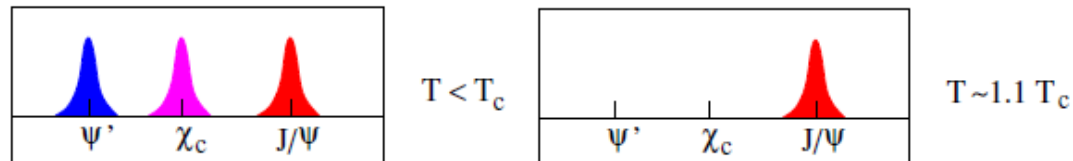
1) The bound states of a heavy quark and its anti-quark

The measured stable charmonium:

the 1S scalar η_c and vector J/ψ , three 1P states χ_c (scalar, vector, and tensor), and the 2S vector state ψ'

2) The different charmonium states melt sequentially as a function of their binding strength;

the most loosely bound state disappears first, the ground state last



H. Satz, J. Phys. G.
32, R25 (2006)

May 16th 2015
an National University

– J/ψ suppression and Debye screening

T. Matsui and H. Satz, Phys. Lett. **B178** 416 (1986)

1) At $T > T_C$ color charges are Debye screened in QGP

$$V = -\frac{4}{3} \frac{\alpha_s}{r} \rightarrow V = -\frac{4}{3} \frac{\alpha_s}{r} e^{-r/\lambda_D} \quad \lambda_D = \frac{1}{gT \sqrt{\frac{N_c}{3} + \frac{N_f}{6}}}$$

Compared to the Bohr radius r_B , the Debye screening prevents the formation of the bound states when $r_B > \lambda_D$

2) The measure for the effect of the quark-gluon plasma on the J/ψ suppression : the nuclear modification factor

$$R_{AA} = \frac{1}{N_{Coll}} \frac{dN_{J/\psi}^{AA} / d\vec{p}_T}{dN_{J/\psi}^{pp} / d\vec{p}_T} = \frac{\sigma_{inel}^{pp}}{N_{Coll}} \frac{dN_{J/\psi}^{AA} / d\vec{p}_T}{d\sigma_{J/\psi}^{pp} / d\vec{p}_T}$$

Hadron production

– Statistical hadronization

P. Braun-Munzinger, J. Stachel, J. P. Wessels, N. Xu, Phys. Lett. **B344**, 43 (1995)

P. Braun-Munzinger, J. Stachel, J. P. Wessels, N. Xu, Phys. Lett. **B365**, 1 (1996)

1) In a chemically and thermally equilibrated system of non-interacting hadrons, the particle production yield is given by

$$N_i = V_H \frac{g_i}{2\pi^2} \int_0^\infty \frac{p^2 dp}{e^{(E_i - \mu_i)/T_H} \pm 1} \quad E_i = \sqrt{m_i^2 + p_i^2}$$

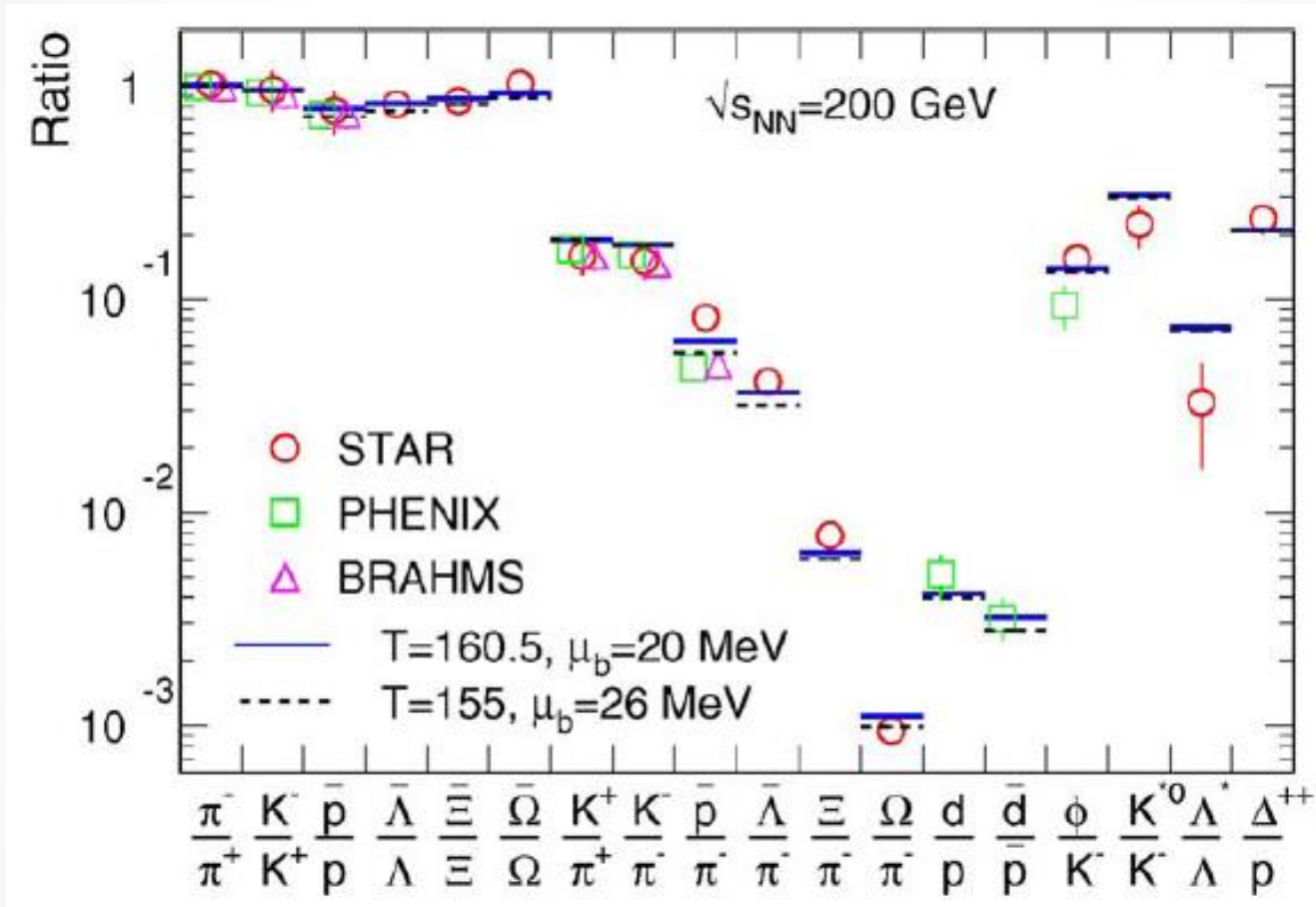
with the chemical potential

$$\mu_i = \mu_B B_i + \mu_{I_3} I_{3i} + \mu_S S_i + \mu_C C_i$$

satisfying $V \sum_i n_i B_i = N_B$, $V \sum_i n_i I_{3i} = I_3^{tot}$, $\sum_i n_i S_i = 0$, and $\sum_i n_i C_i = 0$

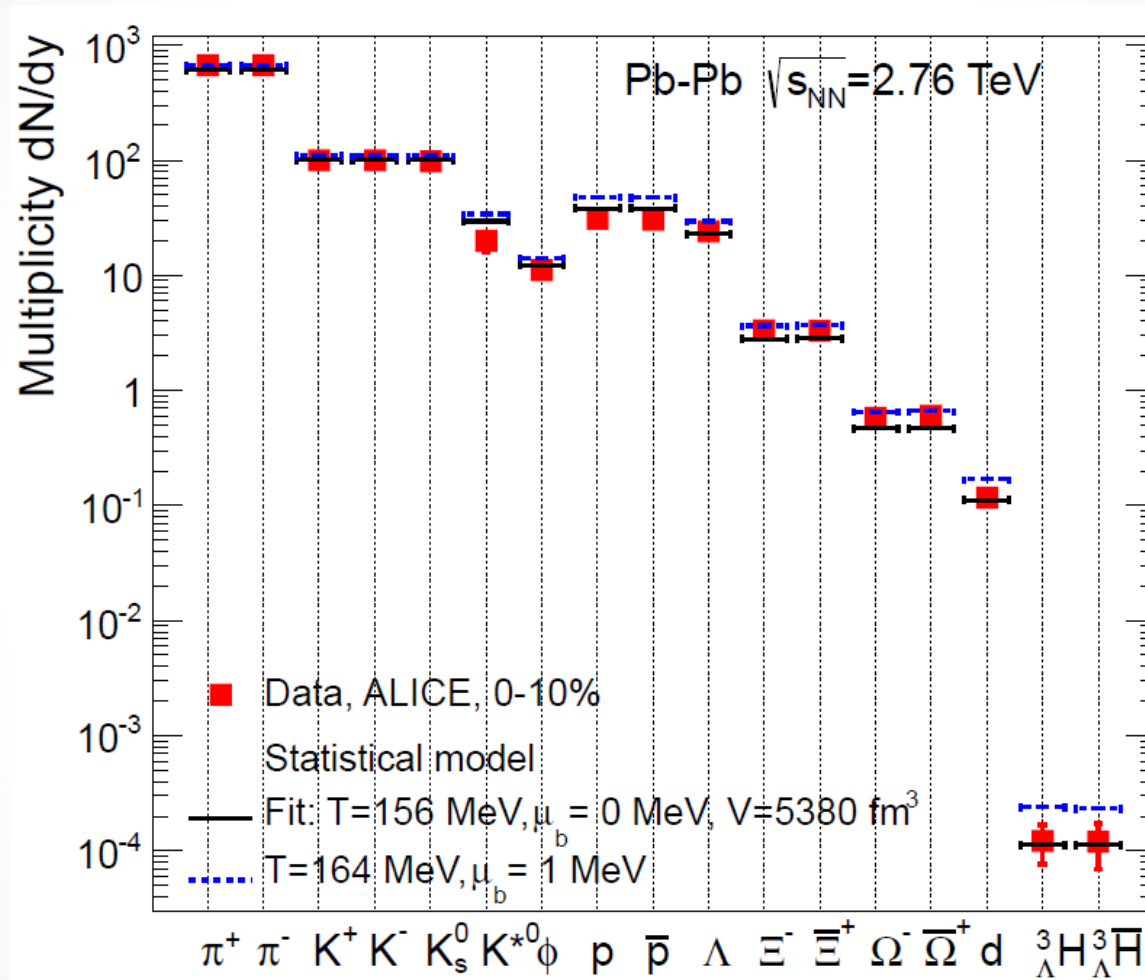
2) The hadronization temperature and the baryon chemical potential should be determined from the experimental data

3) Particle yields ratio at RHIC



A. Andronic, P. Braun-Munzinger, and J. Stachel, Nucl. Phys. A **772**, 167 (2006)

4) Particle yields ratio at LHC



J. Stachel, A. Andronic, P. Braun-Munzinger, and K. Redlich, J. Phys. Conf. Ser. **509**, 012019 (2014)

– Coalescence production of hadrons

1) Covariant coalescence

C. B. Dover, U. Heinz, E. Schnedermann, and J. Zimanyi, Phys. Rev. C **44**, 1636 (1991)

i. A covariant coalescence model for relativistically expanding fireball formed in high-energy nucleus collisions is developed and applied to predict the formation rate of hadrons like deuteron, or pentaquark

ii. Coalescence is basically a non-relativistic phenomenon
The cluster distribution factorizes for arbitrary parent rapidity distributions :

$$\frac{dN_C}{dy} = C \frac{dN_1}{dy} \frac{dN_2}{dy} \quad N_C = CN_1N_2$$

iii. Observation of the antimatter hypernucleus

| Particle type | Ratio |
|--|--------------------------|
| $\frac{3\bar{H}}{\Lambda} / \frac{3H}{\Lambda}$ | $0.49 \pm 0.18 \pm 0.07$ |
| $\frac{3\bar{He}}{\Lambda} / \frac{3He}{\Lambda}$ | $0.45 \pm 0.02 \pm 0.04$ |
| $\frac{3\bar{H}}{\Lambda} / \frac{3\bar{He}}{\Lambda}$ | $0.89 \pm 0.28 \pm 0.13$ |
| $\frac{3H}{\Lambda} / \frac{3He}{\Lambda}$ | $0.82 \pm 0.16 \pm 0.12$ |

B. Abelev *et al.* [The STAR Collaboration], Science, **328**, 58 (2010)

2) The puzzle in antiproton/pion ratio

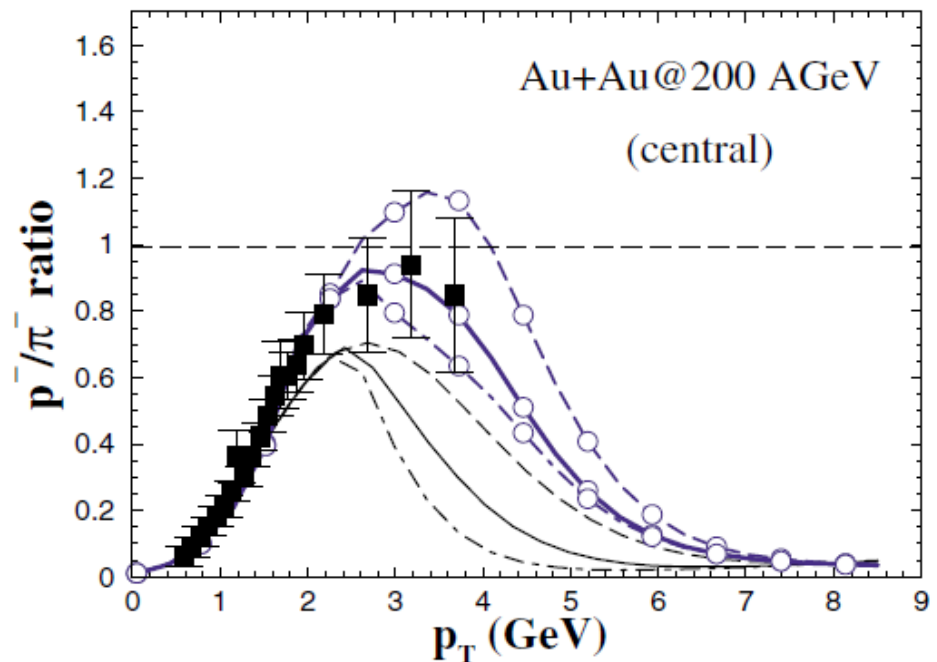
V. Greco, C. M. Ko, and P. Levai, Phys. Rev. Lett. **90**, 202302 (2003)

R. J. Freis, B. Muller, C. Nonaka, and S. Bass, Phys. Rev. Lett. **90**, 202303 (2003)

A competition between two particle production mechanisms

: A fragmentation dominates at large transverse momenta and a coalescence prevails at lower transverse momenta

$$p_T^{Frag} = \frac{p_T^h}{z} \quad \text{vs.} \quad p_T^{Coal} = \frac{p_T^h}{n}$$



3) Quark number scaling of the elliptic flow

Denes Molnar and Sergei A. Voloshin, Phys. Rev. Lett **91**, 092301 (2003)

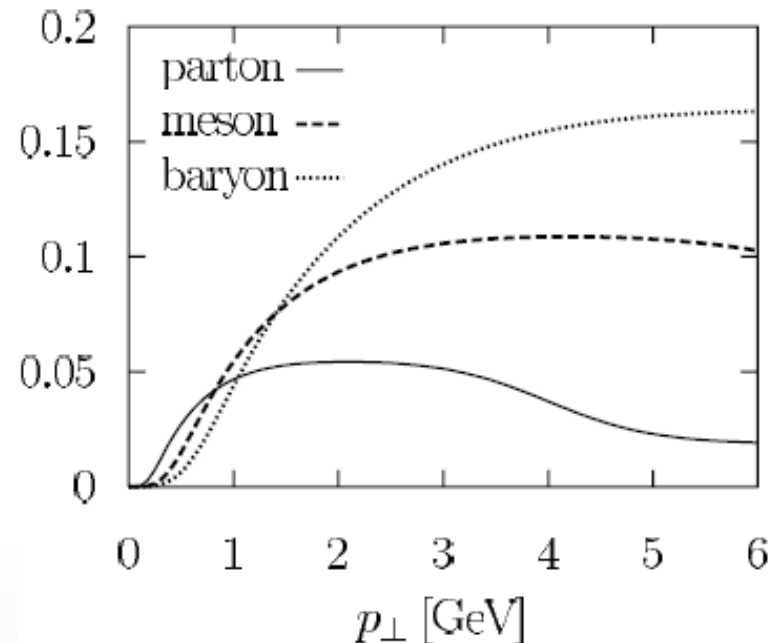
$$v_2(p_T) = \frac{\int d\phi \cos 2\phi \frac{d^2 N}{dp_T^2}}{\int d\phi \frac{d^2 N}{dp_T^2}} \quad \frac{dN_q}{p_T dp_T d\phi} = \frac{1}{2\pi} \frac{dN_q}{p_T dp_T} \left[1 + 2v_{2,q}(p_T) \cos(2\phi) \right]$$

Coalescence model predicts

$$v_{2,M}(p_T) = \frac{2v_{2,q}(p_T/2)}{1 + 2v_{2,q}^2(p_T/2)}$$

$$v_{2,B}(p_T) = \frac{3v_{2,q}(p_T/3) + 3v_{2,q}^3(p_T/3)}{1 + 6v_{2,q}^2(p_T/3)}$$

$$v_{2,h}(p_T) \approx nv_{2,q} \left(\frac{1}{n} p_T \right)$$



4) Yields of hadrons

V. Greco, C. M. Ko, and P. Levai, Phys. Rev. C **68**, 034904 (2003)

R. J. Freis, B. Muller, C. Nonaka, and S. Bass, Phys. Rev. C **68**, 044902 (2003)

$$N^{Coal} = g \int \left[\prod_{i=1}^n \frac{1}{g_i} \frac{p_i \cdot d\sigma_i}{(2\pi)^3} \frac{d^3 p_i}{E_i} f(x_i, p_i) \right] f^W(x_1, \dots, x_n : p_1, \dots, p_n)$$

with the Wigner function, the coalescence probability function

$$\begin{aligned} f^W(x_1, \dots, x_n : p_1, \dots, p_n) \\ = \int \prod_{i=1}^n dy_i e^{p_i y_i} \psi^* \left(x_1 + \frac{y_1}{2}, \dots, x_n + \frac{y_n}{2} \right) \psi \left(x_1 - \frac{y_1}{2}, \dots, x_n - \frac{y_n}{2} \right) \end{aligned}$$

i. A Lorentz-invariant phase space integration of a space-like hypersurface constrains the number of particles in the system

$$\int p_i \cdot d\sigma_i \frac{d^3 p_i}{(2\pi)^3 E_i} f(x_i, p_i) = N_i$$

ii. The transverse momentum spectra

$$\frac{dN_M}{d^2\mathbf{p}_T} = g_M \frac{6\pi}{\tau\Delta y R_\perp^2 \Delta_p^3} \int d^2\mathbf{p}_{1T} d^2\mathbf{p}_{2T} \left. \frac{dN_q}{d^2\mathbf{p}_{1T}} \right|_{|y_1| \leq \Delta y/2} \left. \frac{dN_{\bar{q}}}{d^2\mathbf{p}_{2T}} \right|_{|y_2| \leq \Delta y/2} \\ \times \delta^{(2)}(\mathbf{p}_T - \mathbf{p}_{1T} - \mathbf{p}_{2T}) \Theta(\Delta_p^2 - \frac{1}{4}(\mathbf{p}_{1T} - \mathbf{p}_{2T})^2 - \frac{1}{4}[(m_{1T} - m_{2T})^2 - (m_1 - m_2)^2]).$$

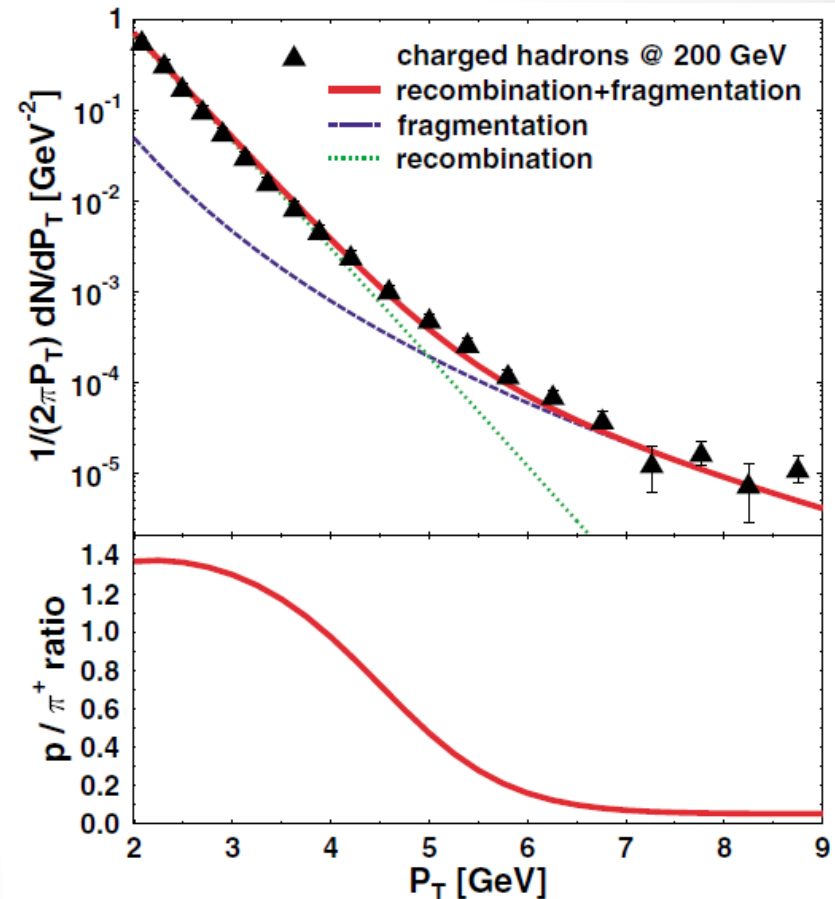
$$f_M(x_1, x_2; p_1, p_2) = \frac{9\pi}{2(\Delta_x \Delta_p)^3} \Theta(\Delta_x^2 - (x_1 - x_2)^2) \\ \times \Theta(\Delta_p^2 - \frac{1}{4}(p_1 - p_2)^2 + \frac{1}{4}(m_1 - m_2)^2).$$

and

$$E \frac{dN_M}{d^3P} = C_M \int_\Sigma \frac{d^3RP \cdot u(R)}{(2\pi)^3} \int \frac{d^3q}{(2\pi)^3} \\ \times w_a\left(R; \frac{\mathbf{P}}{2} - \mathbf{q}\right) \Phi_M^W(\mathbf{q}) w_b\left(R; \frac{\mathbf{P}}{2} + \mathbf{q}\right)$$

$$\Phi_M^W(\mathbf{q}) = \int d^3r \Phi_M^W(\mathbf{r}, \mathbf{q})$$

$$\Phi_M^W(\mathbf{r}, \mathbf{q}) = \int d^3r' e^{-i\mathbf{q}\cdot\mathbf{r}'} \varphi_M\left(\mathbf{r} + \frac{\mathbf{r}'}{2}\right) \varphi_M^*\left(\mathbf{r} - \frac{\mathbf{r}'}{2}\right)$$



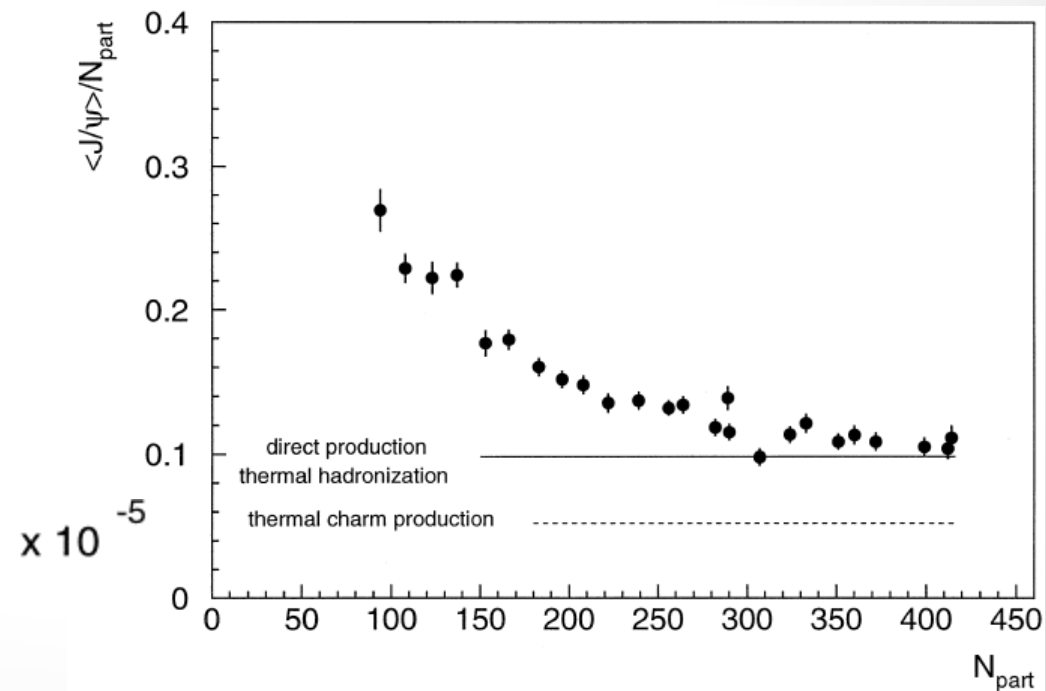
Charmonium states in heavy ion collisions

– Statistical hadronization of J/ψ mesons

P. Braun-Munzinger and J. Stachel, Phys. Lett. **B490**, 196 (2000)

1) All $c\bar{c}$ pairs are produced in direct, hard collisions. Charmed hadron production proceeds through a state of chemical equilibrium near or at the phase boundary

i. The yield of directly produced charm is slightly larger than that produced if charm is in full chemical equilibrium



– Charmonium production in heavy ion collisions

1) Charmonium production ratios versus statistical predictions

| Ratio | $\psi'/(J/\psi)$ | $\chi_{c1}/(J/\psi)$ | $\chi_{c2}/(J/\psi)$ |
|--------------|------------------|----------------------|----------------------|
| Experimental | 0.23 | 1.06 | 1.50 |
| Statistical | 0.045 | 0.113 | 0.148 |

H. Satz, J. Phys. G. **32**, R25 (2006)

2) The production yield ratio between the J/ψ and the ψ'

| T | 160 | 170 | 180 |
|------------------------|--------|--------|--------|
| $dN_{J/\psi}/dy$ | 0.0111 | 0.0106 | 0.0103 |
| $N_{\psi'}/N_{J/\psi}$ | 0.031 | 0.037 | 0.045 |

A. Andronic, P. Braun-Munzinger, K. Redlich, and J. Stachel, Phys. Lett. B **571**, 36 (2003)

3) Statistical Hadronization of charmed mesons

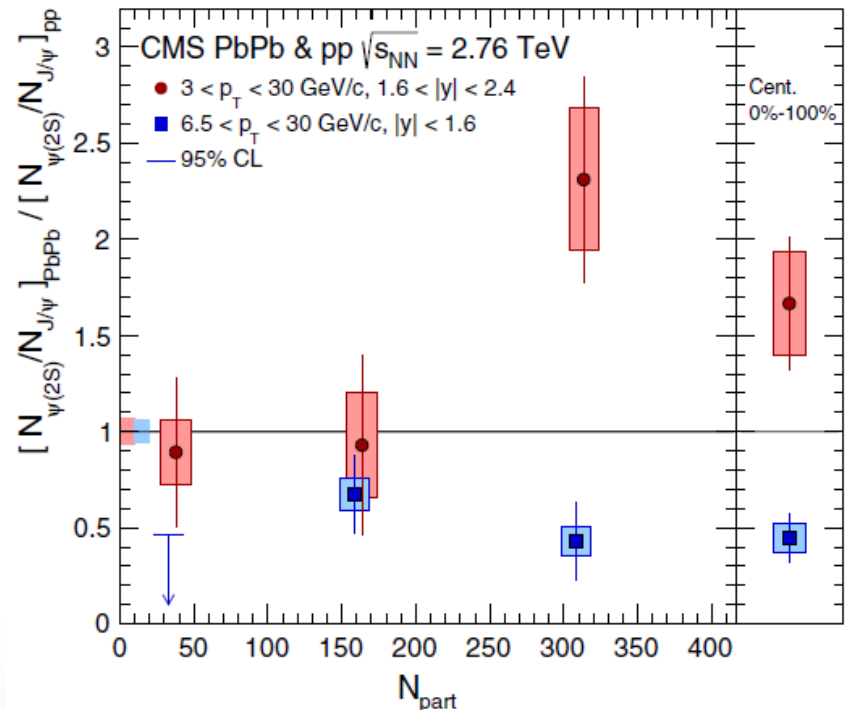
$$N_i = V_H \frac{g_i}{2\pi^2} \int_0^\infty \frac{p^2 dp}{\gamma_i^{-1} e^{E_i/T_H} \pm 1} \quad \gamma_c = 6.40$$

S. Cho et al, (EXHIC Collaboration), Phys. Rev. Lett. **106**, 212001

$$\frac{N_{\psi(2S)}}{N_{J/\psi(2S)} + 0.603N_{\psi(2S)} + 0.348N_{\chi_{c1}} + 0.198N_{\chi_{c2}}} = 0.040$$

4) The production yield ratio between the J/ψ and the ψ'

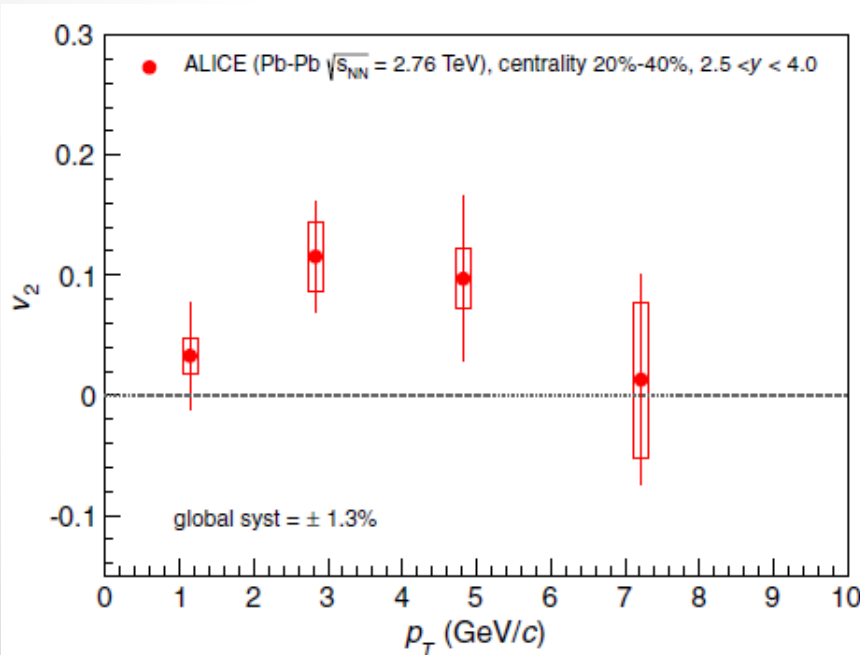
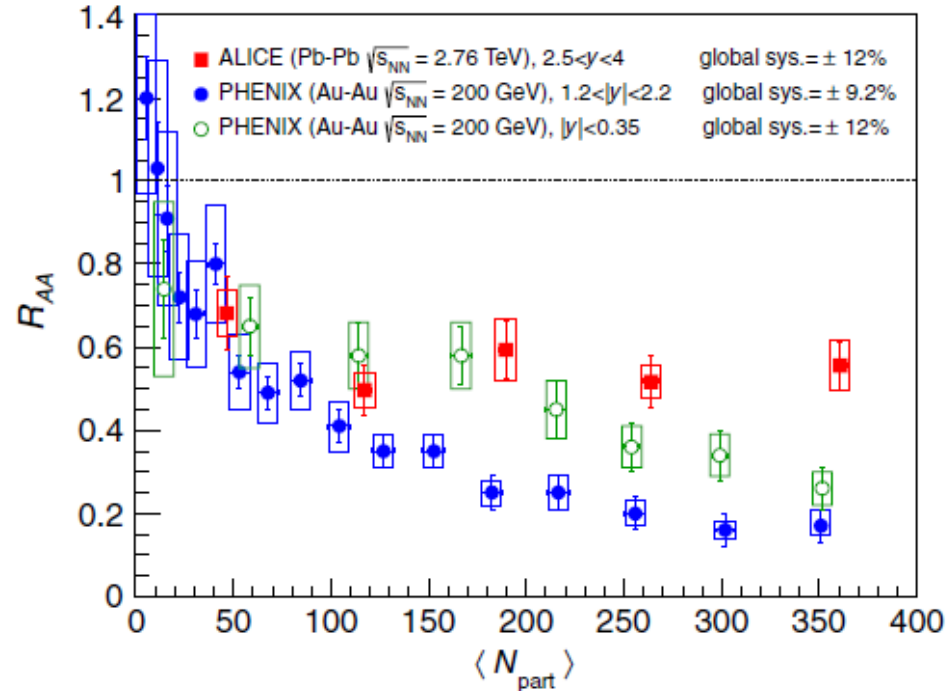
V. Khachatryan et al,
Phys. Rev. Lett. **113**, 262301 (2014)



– Regeneration of J/ψ mesons

1) The nuclear modification factor of J/ψ mesons

B. Abelev et al, (ALICE Collaboration),
Phys. Rev. Lett. **109**, 072301



2) Elliptic flow of the J/ψ

E. Abbas et al, Phys. Rev. Lett. **111**, 162301 (2013)

– Charmonium production by recombination

1) Coalescence production of charmonia - PYTHIA

$$\frac{d^2 N_M}{d\mathbf{p}_T^2} = g_M \int \prod_{i=1}^2 \frac{p_i \cdot d\sigma_i d^3 \mathbf{p}_i}{(2\pi)^3 E_i} f_q(x_1, p_1) f_{\bar{q}}(x_2, p_2) \\ \times f_M(x_1, p_1; x_2, p_2) \delta^{(2)}(\mathbf{p}_T - \mathbf{p}_{1T} - \mathbf{p}_{2T})$$

Number of charmonia produced from charm-quark coalescence at mid-rapidity in central collisions of Au + Au at $\sqrt{s} = 200$ GeV

| | $N_{J/\psi}$ | N_{χ_c} | $N_{\psi'}$ |
|--------|----------------------|----------------------|----------------------|
| PYTHIA | 0.8×10^{-3} | 0.5×10^{-4} | 0.2×10^{-4} |

V. Greco, C. M. Ko, and R. Rapp, Phys. Lett. B **595**, 202 (2004)

2) The transverse momentum distribution of the charmonium yield

$$N_\psi = g_\psi \int p_c \cdot d\sigma_c p_{\bar{c}} \cdot d\sigma_{\bar{c}} \frac{d^3 \vec{p}_c}{(2\pi)^3 E_c} \frac{d^3 \vec{p}_{\bar{c}}}{(2\pi)^3 E_{\bar{c}}} f_c(r_c, p_c) f_{\bar{c}}(r_{\bar{c}}, p_{\bar{c}}) W_\psi(r_c, r_{\bar{c}}; p_c, p_{\bar{c}}),$$

$$\frac{dN_\psi}{d^2 \vec{p}_T} = \frac{g_\psi}{V} \int d^3 \vec{r} d^2 \vec{p}_{cT} d^2 \vec{p}_{\bar{c}T} \delta^{(2)}(\vec{p}_T - \vec{p}_{cT} - \vec{p}_{\bar{c}T}) \frac{dN_c}{d^2 \vec{p}_{cT}} \frac{dN_{\bar{c}}}{d^2 \vec{p}_{\bar{c}T}} W_\psi(\vec{r}, \vec{k})$$

V. Greco, C. M. Ko, and P. Levai, Phys. Rev. C **68**, 034904 (2003)

2) Gaussian Wigner functions for different charmonium states

$$\begin{aligned}
 W_s(\vec{r}, \vec{k}) &= 8e^{-\frac{r^2}{\sigma^2} - k^2\sigma^2} & W_{\psi_{10}}(\vec{r}, \vec{k}) &= \frac{16}{3} \left(\frac{r^4}{\sigma^4} - 2\frac{r^2}{\sigma^2} + \frac{3}{2} - 2\sigma^2 k^2 + \sigma^4 k^4 \right. \\
 W_p(\vec{r}, \vec{k}) &= \left(\frac{16}{3} \frac{r^2}{\sigma^2} - 8 + \frac{16}{3} \sigma^2 k^2 \right) e^{-\frac{r^2}{\sigma^2} - k^2\sigma^2} & & \left. - 2r^2 k^2 + 4(\vec{r} \cdot \vec{k})^2 \right) e^{-\frac{r^2}{\sigma^2} - k^2\sigma^2}.
 \end{aligned}$$

3) Coulomb Wigner functions S. Cho, arXiv: 1408.4756

$$\begin{aligned}
 W_\psi(\vec{r}, \vec{k}) &= \int d^3\vec{q} \psi^*(\vec{r} + \vec{q}/2) e^{i\vec{k} \cdot \vec{q}} \psi(\vec{r} - \vec{q}/2) \\
 &= \int \frac{d^3\vec{q}}{(2\pi)^3} \tilde{\psi}^*(\vec{k} + \vec{q}/2) e^{-i\vec{r} \cdot \vec{q}} \tilde{\psi}(\vec{k} - \vec{q}/2),
 \end{aligned}$$

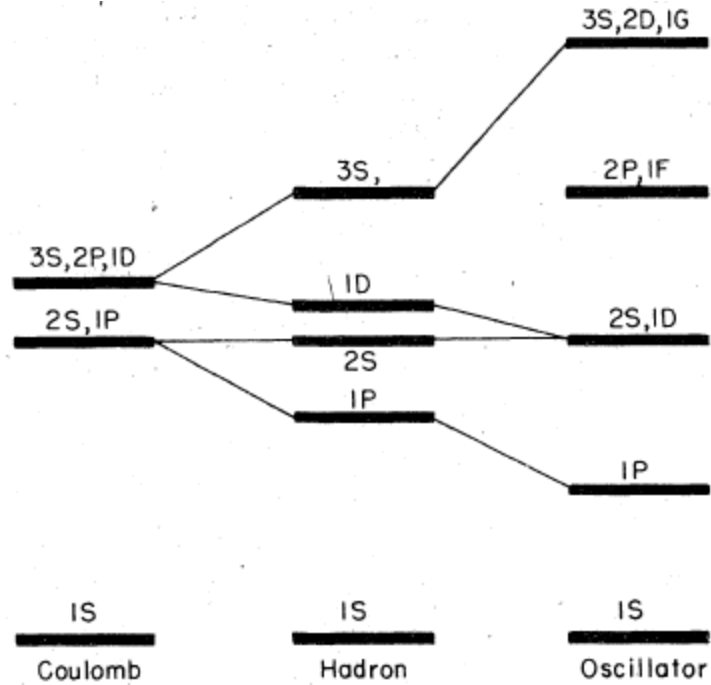
$$W_{\psi_{1S}}(\vec{r}, \vec{k}) = \frac{16}{a_0^5} \int_0^1 du u(1-u) e^{-2i(1-2u)\vec{k} \cdot \vec{r}} e^{-2rC(u)} \left(\frac{3}{C(u)^5} + \frac{6}{C(u)^4} r + \frac{4}{C(u)^3} r^2 \right),$$

$$C(u) = (1/a_0^2 + 4u(1-u)k^2)^{1/2}$$

$$\begin{aligned}
 W_{\psi_{2S}}(\vec{r}, \vec{k}) &= \frac{1}{32a_0^9} \int_0^1 du u^2(1-u)^2 e^{-2i(1-2u)\vec{k} \cdot \vec{r}} \left(\frac{105}{D(u)^9} + \frac{210}{D(u)^8} r + \frac{180}{D(u)^7} r^2 + \frac{80}{D(u)^6} r^3 + \frac{16}{D(u)^5} r^4 \right) e^{-2rD(u)} \\
 &\quad - \frac{1}{4a_0^7} \int_0^1 du u(1-u) e^{-2i(1-2u)\vec{k} \cdot \vec{r}} \left(\frac{15}{D(u)^7} + \frac{30}{D(u)^6} r + \frac{24}{D(u)^5} r^2 + \frac{8}{D(u)^4} r^3 \right) e^{-2rD(u)} \\
 &\quad + \frac{2}{a_0^5} \int_0^1 du u(1-u) e^{-2i(1-2u)\vec{k} \cdot \vec{r}} \left(\frac{3}{D(u)^5} + \frac{6}{D(u)^4} r + \frac{4}{D(u)^3} r^2 \right) e^{-2rD(u)},
 \end{aligned}$$

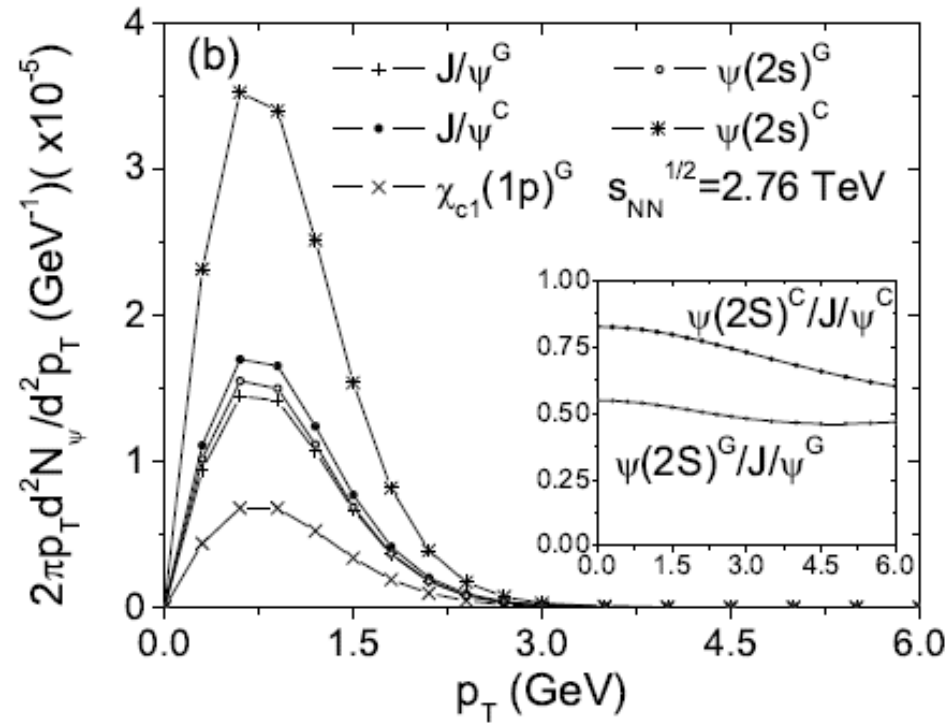
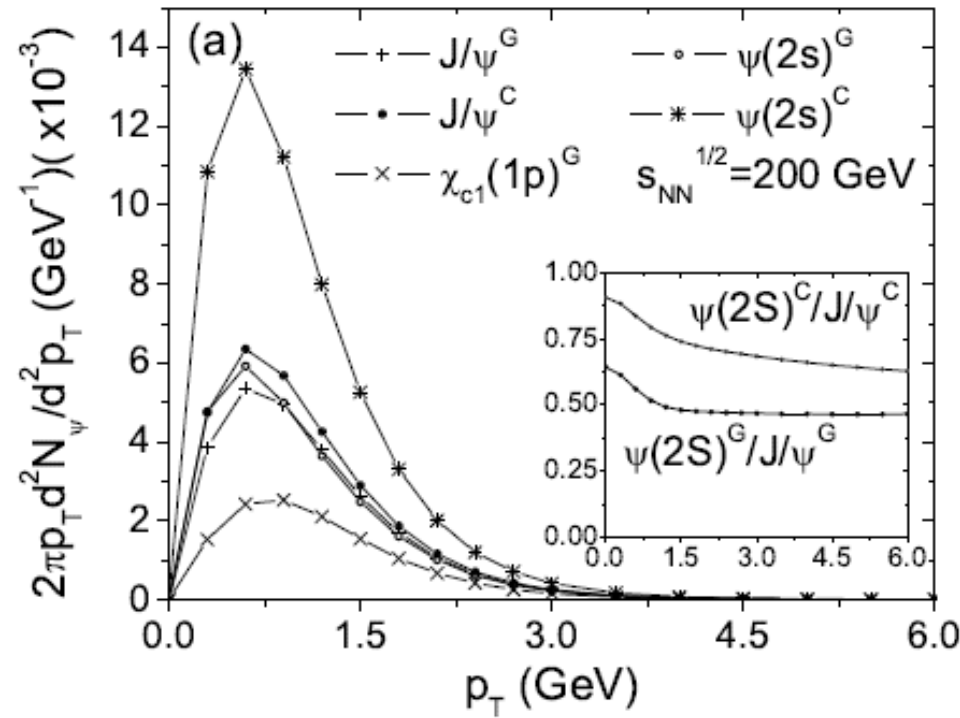
$$\bullet H(D(u)) = (1/(2a_0)^2 + 4u(1-u)k^2)^{1/2}$$

4) Charmonium wave functions



E. Eichten, K. Gottfried, T. Kinoshita, K. D. Lane, T-M, Yan, Phys. Rev. D **17**, 3090 (1978)

5) Transverse momentum distributions



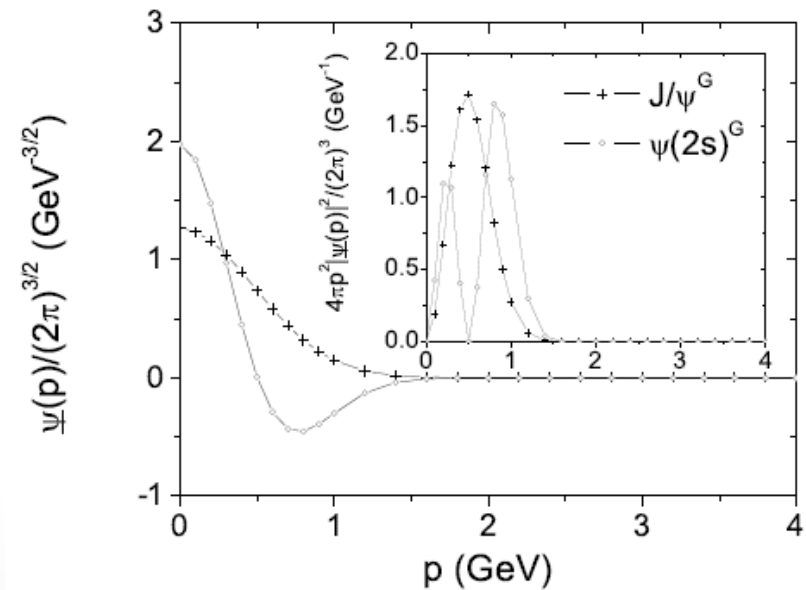
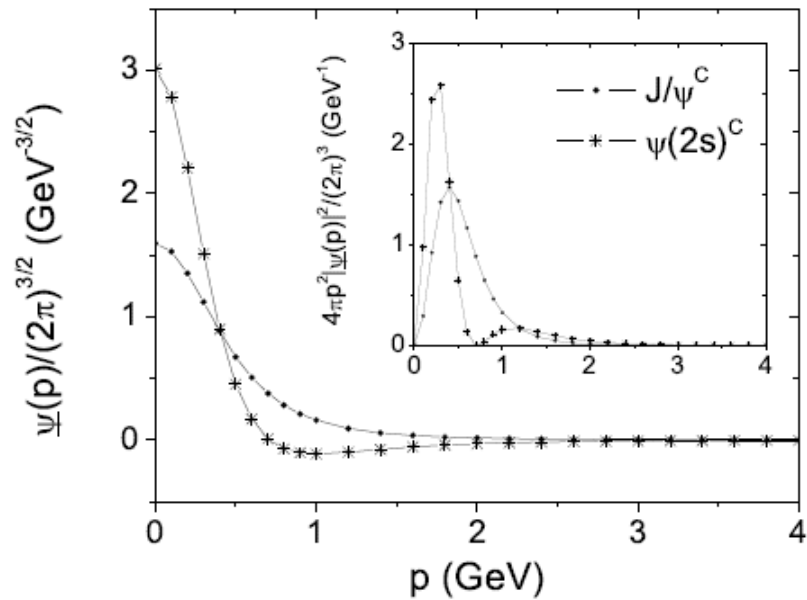
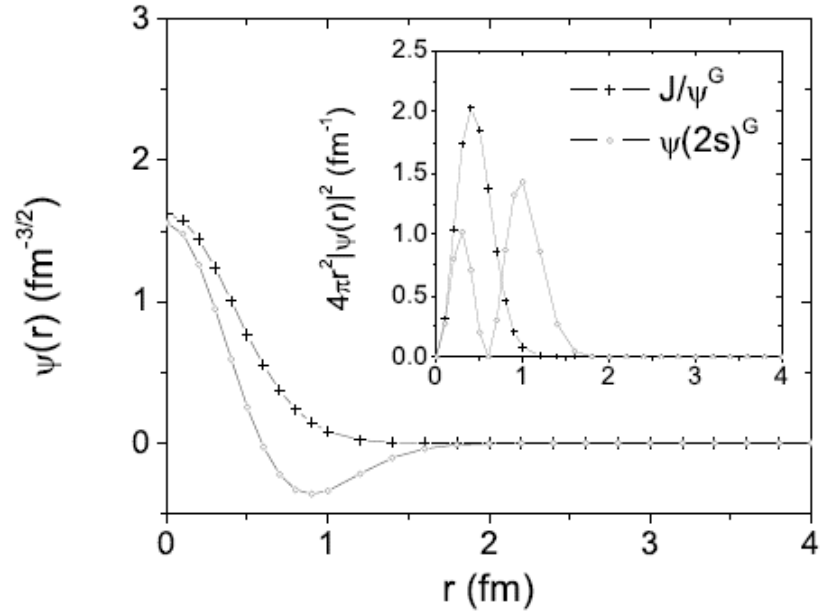
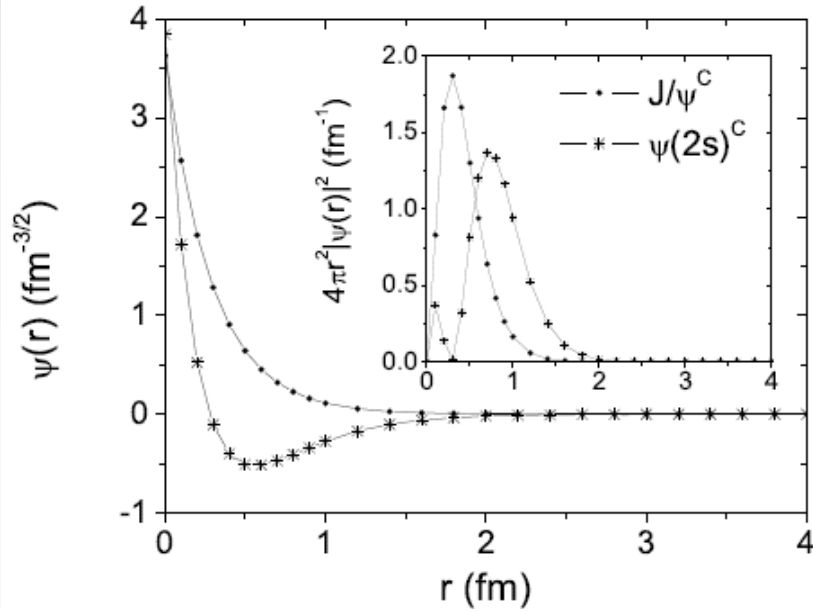
6) Integration of the Wigner function over the spatial coordinates

$$\int d^3\vec{r} W_\psi(\vec{r}, \vec{k}) = \begin{cases} (2\sqrt{\pi}\sigma)^3 e^{-k^2\sigma^2} & \psi_s^G; J/\psi \\ \frac{2}{3}(2\sqrt{\pi}\sigma)^3 e^{-k^2\sigma^2} \sigma^2 k^2 & \psi_p^G; \chi_c \\ \frac{2}{3}(2\sqrt{\pi}\sigma)^3 e^{-k^2\sigma^2} \left(\sigma^2 k^2 - \frac{3}{2}\right)^2 & \psi_{10}^G; \psi(2S) \\ 64\pi \frac{a_0^3}{(a_0^2 k^2 + 1)^4} & \psi_{1S}^C; J/\psi \\ 8\pi a_0^3 \frac{(a_0^2 k^2 - 1/4)^2}{(a_0^2 k^2 + 1/4)^6} & \psi_{2S}^C; \psi(2S) \end{cases}$$

$$\int d^3\vec{r} W(\vec{r}, \vec{p}) = |\varphi(\vec{p})|^2$$

M. Hillery, R. F. O'Connell, M. O. Scully and E. P. Wigner, Phys. Rept. **106**, 121 (1984)

7) Wave function distributions



Conclusion

- Production of charmonium states in heavy ion collisions
- 1) Light quark hadron yields are well explained by the statistical hadronization model
 - 2) Many aspects of the heavy ion collision experimental results have been explained by the coalescence model
 - 3) The production of heavy quarks hadrons, or charmonium can also be understood by the coalescence model
 - 4) The enhanced transverse momentum distribution of $\psi(2S)$ mesons compared to that of J/ψ mesons, originated from intrinsic wave function distributions of $\psi(2S)$ and J/ψ mesons, provides a plausible explanation for the measurement of the nuclear modification factor ratio between the $\psi(2S)$ and J/ψ meson.